

Simultaneous metal-insulator and spin-state transitions in $\text{Pr}_{0.5}\text{Ca}_{0.5}\text{CoO}_3$

Shingo Tsubouchi,¹ Tôru Kyômen,¹ Mitsuru Itoh,^{1,*} Parthasarthy Ganguly,^{1,†} Masaharu Oguni,² Yutaka Shimojo,³
Yukio Morii,³ and Yoshinobu Ishii³

¹Materials and Structures Laboratory, Tokyo Institute of Technology, 4259 Nagatsuta, Midori-ku, Yokohama 226-8503, Japan

²Department of Chemistry, Graduate School of Science and Engineering, Tokyo Institute of Technology, 2-12-1 Ookayama, Meguro-ku,
Tokyo 152-8551, Japan

³Advanced Science Research Center, Japan Atomic Energy Research Institute, Tokai, Ibaraki 319-1195, Japan

(Received 27 June 2002; published 29 August 2002)

$\text{Pr}_{0.5}\text{Ca}_{0.5}\text{CoO}_3$ showed a simultaneous metal-insulator and paramagnetic-paramagnetic spin-state transition of the first-order type at 90 K accompanied by a volume contraction by $\sim 2\%$. Neutron diffraction analysis revealed that the volume contraction is mainly attributed to the tilting of CoO_6 octahedra which causes a decrease in the Co-O-Co angle. The electron configurations were proposed to be localized t_{2g}^6 (trivalent Co) and t_{2g}^5 (tetravalent Co) in the low-temperature phase and itinerant $t_{2g}^5 e_g^{0.5}$ in the high-temperature phase.

DOI: 10.1103/PhysRevB.66.052418

PACS number(s): 75.30.-m, 71.70.Ej, 71.30.+h

A temperature-induced low-spin to high-spin transition is well known in some transition-metal complexes such as $\text{Fe}(\text{phen})_2(\text{NCS})_2$.¹ Similar transitions have been reported to occur in certain perovskite-related cobalt oxides also. One of these interesting materials is a perovskite oxide LaCoO_3 , whose ground state is the low-spin state t_{2g}^6 .^{2,3} The magnetic susceptibility shows Curie-Weiss behavior with a Curie constant $2 \text{ emu mol}^{-1} \text{ K}$ above 650 K. The Curie constant gradually changes to $1.3 \text{ emu mol}^{-1} \text{ K}$ between 350 and 110 K which is accompanied by a gradual resistivity change from metal to insulator (semiconductor). Moreover, the magnetic susceptibility decreases to about zero as the temperature decreases after showing a maximum of around 100 K with a large maximum in resistivity. The other interesting materials are oxygen-deficient perovskite oxides $\text{LnBaCo}_2\text{O}_{5+\delta}$ (Ln = rare-earth atom). In $\text{LnBaCo}_2\text{O}_{5.5}$ (Ln = Pr, Sm, Eu, Gd, and Tb), a metal-insulator transition (MIT), paramagnetic-ferromagnetic, and ferromagnetic-antiferromagnetic transitions occur, e.g., around 350, 280, and 200 K, respectively, in the case that Ln = Gd.⁴⁻⁷ The inverse of magnetic susceptibility vs temperature curve shows a clear bend at the MIT temperature, implying a cooperative spin-state transition. In $\text{LnBaCo}_2\text{O}_5$ (Ln = Y and Ho), an antiferromagnetic ordering and a charge ordering of divalent and trivalent Co atoms occur, e.g., around 350 and 220 K, respectively, in the case that Ln = Y.^{8,9} However, Vogt *et al.* have reported that the spin-state changes at the charge ordering temperature in YBaCo_2O_5 ,⁸ while on the other hand, Suard *et al.* have not mentioned it in $\text{HoBaCo}_2\text{O}_5$.⁹

The electronic state, low-spin or high-spin state, of the transition metal ion with d^n ($n = 4, 5, 6,$ and 7) configuration in transition-metal complexes is determined by the two competing energies, crystal field energy, and Hund coupling energy.¹ However, it has been proposed that the intermediate-spin state ($t_{2g}^5 e_g^1$ or $t_{2g}^4 e_g^1$) can be the ground state of perovskite oxides with trivalent or tetravalent Co atoms due to the large hybridization with hole on oxygen state ($t_{2g}^5 e_g^2 \underline{L}$ or $t_{2g}^4 e_g^2 \underline{L}$, where \underline{L} indicates hole on oxygen with e_g symmetry).¹⁰⁻¹² This implies that the covalency of

Co and O atoms plays an important role to induce the spin-state transitions. In fact, the spin-state transitions are always accompanied by a change in electrical conductivity associated with the covalency.

$\text{Ln}_{1-x}\text{Sr}_x\text{CoO}_3$ (Ln = La, Pr, Nd, and Sm) perovskite oxides (without oxygen deficiency) are metallic ferromagnets.¹³⁻¹⁶ However, few reports describe $\text{Ln}_{1-x}\text{A}_x\text{CoO}_3$ (A = Ba and Ca).^{17,18} In this paper, we report a material $\text{Pr}_{0.5}\text{Ca}_{0.5}\text{CoO}_3$ showing a temperature-induced paramagnetic-paramagnetic spin-state transition accompanied by a simultaneous MIT. To our knowledge, this is the first report describing both the cooperative MIT and spin-state transition in perovskite cobalt oxides including nearly 50:50 trivalent and tetravalent Co atoms.

Polycrystalline $\text{Pr}_{0.5}\text{Ca}_{0.5}\text{CoO}_3$ was prepared using a conventional solid-state reaction method from Pr_6O_{11} , $\text{CoC}_2\text{O}_4 \cdot 2\text{H}_2\text{O}$, and CaCO_3 . Calcination was carried out in an O_2 gas flow at 1373 K for 12 h twice with intermittent grinding. The calcined powder was pressed into a pellet, sintered in an O_2 gas flow at 1473 K for 24 h, and cooled down to room temperature at a rate 100 K/h. Powder x-ray diffraction (XRD) measurements (Mac science MXP 18-HF system using $\text{CuK}\alpha$ radiation) showed the absence of impurity phases. Iodometric titrations gave the composition as $\text{Pr}_{0.5}\text{Ca}_{0.5}\text{CoO}_{3.02 \pm 0.03}$. The lattice constants were determined in the range of 30–297 K from the XRD data using crystalline silicon as an internal standard. In order to determine the precise crystal and magnetic structures, powder neutron diffraction (ND) measurements were carried out using a high resolution powder diffractometer (HRPD) at 10 and 297 K in JAERI, Tokai, Japan. The wavelength of neutrons is 1.82418(5) Å. Rietveld refinements of the ND data were carried out by using the RIETAN-2000 program.¹⁹ Resistivities were measured in the range of 2–350 K by a standard dc four-probe method using the Physical Property Measurement System (PPMS, Quantum Design). dc magnetizations were measured in the range of 2–345 K with a superconducting quantum interference device magnetometer (MPMS5S, Quantum Design). Heat capacities were measured in the range of 13–300 K using an adiabatic method employing a

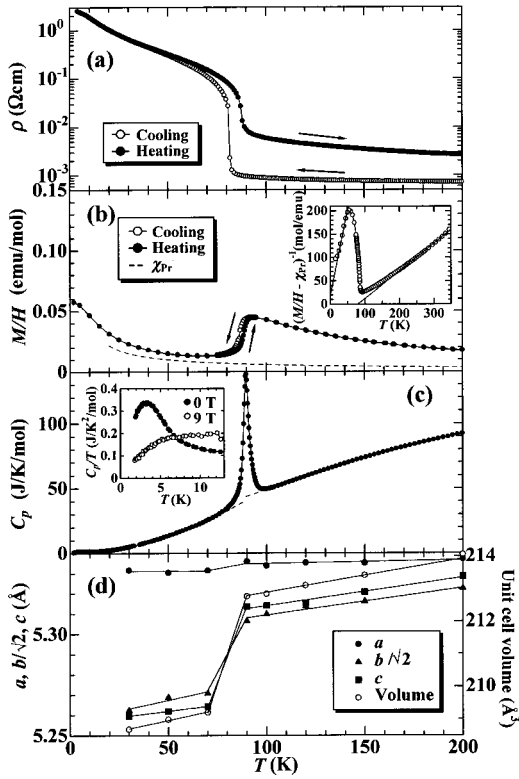


FIG. 1. (a) Resistivities, (b) dc magnetizations, (c) heat capacities, and (d) lattice constants and unit cell volume of $\text{Pr}_{0.5}\text{Ca}_{0.5}\text{CoO}_3$. The error bars of lattice constants and unit cell volume are in the order of the mark size. The inset of (b) shows the inverse of contribution to magnetic susceptibility from Co atoms obtained by subtracting Pr contributions [dashed line in (b)]. The solid lines in the inset indicate the results of fitting according to Curie-Weiss law. The inset of (c) shows the C_p/T vs T plot in magnetic fields 0 and 9 T. The other solid lines on the marks are visual guides.

high-precision adiabatic calorimeter²⁰ and in the range of 1.8–13 K and in the magnetic fields 0 and 9 T using a relaxation method employing PPMS.

The resistivity of the sample was measured on cooling from 350 to 5 K and successively on heating from 5 to 350 K as shown in Fig. 1(a). The resistivity ($T > 100$ K) on cooling is considerably less than the value of 2 mΩ cm that has been universally observed¹³ as the maximum limiting value of the resistivity for the metallic perovskite oxide system. There is an abrupt increase (by nearly two orders of magnitude) in the resistivity on cooling below 80 K. This abrupt change in resistivity was observed also in the heating measurements but the temperature rose (90 K), characteristic of a first-order transition. Another feature is that the resistivity value on heating is markedly larger than that on cooling for $T > 50$ K. The origin of this irreversibility in the resistivity is likely to be due to some extrinsic experimental artifact associated with electrical connectivity (e.g., formation of cracking due to the large volume change described below) rather than some intrinsic cause, since the magnetization behavior shows no such effect (see below).

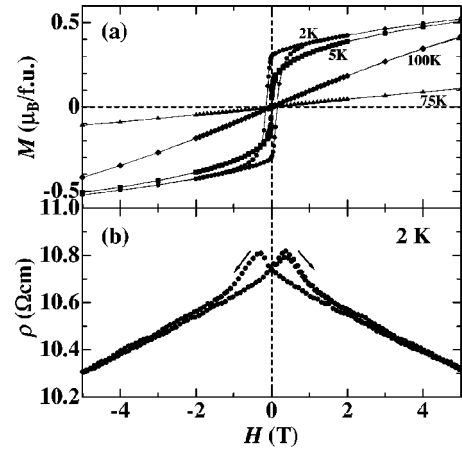


FIG. 2. (a) dc magnetization per formula unit to magnetic field curves at 2, 5, 75, and 100 K. (b) Resistivity to magnetic field curve at 2 K. The magnetic field was scanned in the order of $0 \rightarrow 5 \rightarrow -5 \rightarrow 5$ T. Solid lines are visual guides.

In Fig. 1(b), the dc magnetization M measured at an external magnetic field $H (= 5$ T) is plotted as M/H against temperature. The magnetization decreases abruptly on cooling below ~ 90 K, and a small hysteresis (~ 2 K) is seen in the heating and cooling cycles near the transition point. Pr's contribution to the magnetic susceptibility was subtracted out (tentatively using the data of Ref. 21) in order to evaluate the net contribution of the Co atoms. This is shown in the inset of Fig. 1(b). The high-temperature susceptibility from the Co atoms ($T > 200$ K) shows a Curie-Weiss behavior typical of a ferromagnet with a Curie constant of $1.7 \text{ emu mol}^{-1} \text{ K}$, comparable to $1.8 \text{ emu mol}^{-1} \text{ K}$ for a metallic ferromagnet $\text{La}_{0.5}\text{Sr}_{0.5}\text{CoO}_3$.¹⁴ The Curie constant increased below 200 K, indicating formation of giant moments by a short-range ferromagnetic coupling among Co atoms. The ferromagnetic coupling was also confirmed by the nonlinearity in the $M-H$ curve at 100 K, as indicated by the solid diamonds in Fig. 2(a), because such a nonlinearity is not observed in antiferromagnet or paramagnet at such a small H/T . The metallicity, Curie constant, and the presence of ferromagnetic interaction in the high-temperature phase suggest that the electronic and spin states are essentially identical to those in the paramagnetic phase of $\text{La}_{0.5}\text{Sr}_{0.5}\text{CoO}_3$.

The absence of magnetic neutron diffraction peaks at 297 and 10 K (not shown) indicates that the sample is a paramagnet in both the high- and low-temperature phases at least down to 10 K. As a result, the contribution of Co atoms to the magnetic susceptibility also obeys a Curie-Weiss law between 50 and 20 K. However, the Curie constant $0.3 \text{ emu mol}^{-1} \text{ K}$ and the paramagnetic Curie temperature ~ 0 K are rather smaller than those of the high-temperature phase. In addition, the $M-H$ curve at 75 K [triangles in Fig. 2(a)] shows nearly linear behavior in spite of showing nonlinear behavior at 100 K. These results indicate that the Co spin state and the mean field at the Co site change at the phase transition. The following results suggest that Co atoms are in the low-spin states (t_{2g}^6 and t_{2g}^5) in the low-temperature phase. $M-H$ and $\rho-H$ results at 2 K showed ferromagnetic

hysteresis loops as indicated by the solid circles in Figs. 2(a) and 2(b). Since electrical conduction is associated with Co atoms, the ferromagnetic ordering cannot be attributed to Pr atoms but to Co atoms. In addition, a heat capacity anomaly was observed around 3 K which is collapsed at a 9 T magnetic field, characteristic of ferromagnets, as shown in the inset of Fig. 1(c). The total entropy at 0 T was calculated to be $2.3 \text{ J K}^{-1} \text{ mol}^{-1}$ by integrating C_p/T in the temperature range 2 to 13 K. Since the lattice contribution to the heat capacity is small at such low temperatures, the entropy originates mainly from the spin ordering. The heat capacity anomaly seems to tail to both high- and low-temperature sides. The sum of the contributions and the entropy estimated between 2 and 13 K would be close to $0.5R \ln 2$ ($= 2.9 \text{ J K}^{-1} \text{ mol}^{-1}$), where R is the gas constant. The coexistence of the low-spin trivalent ($S=0$) and tetravalent ($S=1/2$) Co atoms in the low-temperature phase is consistent not only qualitatively with the small Curie constant and Curie temperature but also quantitatively with the entropy and saturation magnetization ($\sim 0.5\mu_B$).

Heat capacity measurements showed a sharp anomaly around 90 K indicating a cooperative nature. The transition entropy was estimated to be $4.7 \text{ J K}^{-1} \text{ mol}^{-1}$ by assuming the dashed line in Fig. 1(c) as a baseline. The transition entropy is rather smaller than $40\text{--}65 \text{ J K}^{-1} \text{ mol}^{-1}$ of the low-spin to high-spin transition in divalent iron complexes.¹ This indicates that the driving force of transition is different from that of complexes.¹ Senaris-Rodriguez and Goodenough have suggested a $t_{2g}^5 e_g^{*0.5}$ configuration for $\text{La}_{0.5}\text{Sr}_{0.5}\text{CoO}_3$.¹⁴ We also believe that this configuration is the most probable for a metallic phase, since the e_g electron is easily transferred because of the same number of t_{2g} electrons at each Co site. In fact, the combination of trivalent intermediate-spin and tetravalent low-spin in the high-temperature phase corresponding to this configuration gives the transition entropy as $4.6 \text{ J K}^{-1} \text{ mol}^{-1}$ [$= 0.5R(\ln 3 + \ln 2) - 0.5R \ln 2$], which is close to experimental one.

XRD and ND peaks at 297 K can be indexed by the space group $Pnma$. There is no superlattice reflection in both XRD at 30 K and ND at 10 K. The temperature dependence of the lattice constants and unit cell volume are shown in Fig. 1(d). There is an abrupt change in the lattice b and c constants around 90 K with the unit cell volume decreasing by as much as $\sim 2\%$ between 70 and 90 K, which is markedly large as compared with $\sim 0.5\%$ at the MIT of other perovskite oxides.^{22–24} Table I shows the results of Rietveld refinement of ND patterns at 297 and 10 K, and several bond lengths and bond angles calculated from the results. All Co-O bond lengths and O-Co-O bond angles are almost the same between 10 and 297 K. On the other hand, two Co-O-Co bond angles change by as much as $\sim 4^\circ$, which is markedly large as compared with $\sim 1^\circ$ at the MIT's of PrNiO_3 and NdNiO_3 .²⁴ These results conclude that CoO_6 octahedra themselves tilt without deformation at the phase transition and that the large volume change is attributed to the large tilting.

The mean Co-O bond length, 1.921 Å, at 10 K is close to that, 1.924 Å, of LaCoO_3 at 4 K.²⁵ This is consistent with the low-spin states suggested for $\text{Pr}_{0.5}\text{Ca}_{0.5}\text{CoO}_3$. On the other

TABLE I. Structural data of $\text{Pr}_{0.5}\text{Ca}_{0.5}\text{CoO}_3$ ($Pnma$).

	10 K	297 K
a (Å)	5.3279(1)	5.340 45(7)
b (Å)	7.4576(1)	7.540 61(9)
c (Å)	5.2616(1)	5.337 66(7)
V (Å ³)	209.058(7)	214.949(5)
$B(\text{Co}; 4b)$ (Å ²)	0.2(1)	0.5(1)
$x[\text{O}(1); 4c]$	-0.0143(2)	-0.0080(3)
$z[\text{O}(1); 4c]$	0.5802(2)	0.5672(3)
$B[\text{O}(1); 4c]$ (Å ²)	0.3(1)	0.6(1)
$x[\text{O}(2); 8d]$	0.2934(1)	0.2847(2)
$y[\text{O}(2); 8d]$	0.0408(1)	0.0344(1)
$z[\text{O}(2); 8d]$	0.2952(2)	0.2857(2)
$B[\text{O}(2); 8d]$ (Å ²)	0.3(1)	0.6(1)
R_{wp}	5.40%	4.43%
R_I	1.19%	2.18%
Co-O(1) (Å)	1.9131(3)	1.9194(3)
Co-O(2) (Å)	1.9228(7)	1.921(1)
	1.9279(7)	1.927(1)
$\angle \text{O}(2)\text{-Co-O}(2)$ (°)	90.70(1)	90.99(1)
$\angle \text{O}(1)\text{-Co-O}(2)$ (°)	90.07(5)	90.12(7)
	90.10(4)	90.22(6)
$\angle \text{Co-O}(1)\text{-Co}$ (°)	154.10(7)	158.3(1)
$\angle \text{Co-O}(2)\text{-Co}$ (°)	152.97(4)	157.73(6)

hand, the mean Co-O bond length 1.922 Å at 297 K is nearly the same as that at 10 K. At first glance, this seems to contradict the occurrence of spin-state transition at 90 K, because the mean Fe-N bond length in divalent iron complexes changes by 0.16–0.22 Å at the low-spin to high-spin transition.¹ However, this is not strange, because the mean Co-O bond length 1.931 Å of $\text{La}_{0.5}\text{Sr}_{0.5}\text{CoO}_3$ at room temperature¹⁵ is close to that of LaCoO_3 at 4 K. The Co-O bond length in the high-temperature phase is supposed to be decreased from the ionic bond length by the strong covalency. The remarkable change in Co-O-Co bond angles has been also reported in carrier doping induced MIT in $\text{La}_{1-x}\text{Sr}_x\text{CoO}_3$ around $x=0.2$.¹⁵ In the low-temperature phase, the large decrease of the Co-O-Co bond angle results in a reduction of the covalency and thus would destabilize the itinerant intermediate-spin state as explained by Potze and Korotin *et al.*^{11,12} In addition, the large volume contraction enlarges the splitting of the crystal field, leading to a stabilization of the localized low-spin state. These observations are consistent with our suggestion.

In conclusion, we have reported a simultaneous metal-insulator and paramagnetic-paramagnetic spin-state transition in $\text{Pr}_{0.5}\text{Ca}_{0.5}\text{CoO}_3$ accompanied by large changes in unit cell volume and Co-O-Co bond angles. The electron configurations were proposed to be localized t_{2g}^6 (trivalent Co) and t_{2g}^5 (tetravalent Co) in the low-temperature phase and itinerant $t_{2g}^5 e_g^{0.5}$ in the high-temperature phase. The connectivity of the spin-state transition with the MIT, relatively small transition entropy, and no remarkable change in Co-O bond lengths are different in nature from the low-spin to

high-spin transition in transition-metal complexes, while on the other hand, the large volume change is similar to the complexes. The appearance/disappearance of e_g electrons would constitute the primary origin of the MIT. However, it is necessary to further investigate the possible existence of

charge/orbital ordering as another possible candidate for the MIT's origin.

Part of this work was financially supported by a Grant-in-Aid for Scientific Research from the Ministry of Education, Science, Culture, and Sports of Japan.

*Author to whom correspondence should be addressed. Electronic address: m.itoh@rlem.titech.ac.jp

†On leave from National Chemical Laboratory, India.

¹P. Gütllich, A. Hauser, and H. Spiering, *Angew. Chem. Int. Ed. Engl.* **33**, 2024 (1994), and references therein.

²M. A. Senaris-Rodriguez and J. B. Goodenough, *J. Solid State Chem.* **116**, 224 (1995).

³K. Asai, A. Yoneda, O. Yokokura, J. M. Tranquada, G. Shirane, and K. Kohn, *J. Phys. Soc. Jpn.* **67**, 290 (1998).

⁴C. Martin, A. Maignan, D. Pelloquin, N. Nguyen, and B. Raveau, *Appl. Phys. Lett.* **71**, 1421 (1997).

⁵A. Maignan, C. Martin, D. Pelloquin, N. Nguyen, and B. Raveau, *J. Solid State Chem.* **142**, 247 (1999).

⁶Y. Moritomo, T. Akimoto, M. Takeo, A. Machida, E. Nishibori, M. Takata, M. Sakata, K. Ohoyama, and A. Nakamura, *Phys. Rev. B* **61**, R13 325 (2000).

⁷T. Saito, T. Arima, Y. Okimoto, and Y. Tokura, *J. Phys. Soc. Jpn.* **69**, 3525 (2000).

⁸T. Vogt, P. M. Woodward, P. Karen, B. A. Hunter, P. Herring, and A. R. Moodenbaugh, *Phys. Rev. Lett.* **84**, 2969 (2000).

⁹E. Suard, F. Fauth, V. Caignaert, I. Mirebeau, and G. Baldinozzi, *Phys. Rev. B* **61**, R11 871 (2000).

¹⁰J. B. Goodenough, *Mater. Res. Bull.* **6**, 967 (1971).

¹¹R. H. Potze, G. A. Sawatzky, and M. Abbate, *Phys. Rev. B* **51**, 11 501 (1995).

¹²M. A. Korotin, S. Yu. Ezhov, I. V. Solovyev, V. I. Anisimov, D. I.

Khomskii, and G. A. Sawatzky, *Phys. Rev. B* **54**, 5309 (1996).

¹³P. Ganguly, P. S. Anil Kumar, P. N. Santhosh, and I. S. Mulla, *J. Phys.: Condens. Matter* **6**, 533 (1994).

¹⁴M. A. Senaris-Rodriguez and J. B. Goodenough, *J. Solid State Chem.* **118**, 323 (1995).

¹⁵A. Mineshige, M. Kobune, S. Fujii, Z. Ogumi, M. Inada, T. Yao, and K. Kikuchi, *J. Solid State Chem.* **142**, 374 (1999).

¹⁶K. Yoshii, H. Abe, and A. Nakamura, *Mater. Res. Bull.* **6**, 1447 (2001).

¹⁷A. V. Samoilov, G. Beach, C. C. Fu, N.-C. Yeh, and R. P. Vasquez, *Phys. Rev. B* **57**, R14 032 (1998).

¹⁸F. Fauth, E. Suard, and V. Caignaert, *Phys. Rev. B* **65**, 060401 (2002).

¹⁹F. Izumi and T. Ikeda, *Mater. Sci. Forum* **321-324**, 198 (2000).

²⁰H. Fujimori and M. Oguni, *J. Phys. Chem. Solids* **54**, 271 (1993).

²¹K. Sekizawa, M. Kitagawa, and Y. Takano, *J. Magn. Magn. Mater.* **177-181**, 541 (1998).

²²H. Kawano, H. Yoshizawa, and Y. Ueda, *J. Phys. Soc. Jpn.* **63**, 2857 (1994).

²³P. G. Radaelli, D. E. Cox, M. Marezio, S.-W. Cheong, P. E. Schiffer, and A. P. Ramirez, *Phys. Rev. Lett.* **75**, 4488 (1995).

²⁴J. L. Garcia-Munoz, J. Rodriguez-Carvajal, P. Lacorre, and J. B. Torrance, *Phys. Rev. B* **46**, 4414 (1992).

²⁵G. Thornton, B. C. Tofield, and A. W. Hewat, *J. Solid State Chem.* **61**, 301 (1986).